ELSEVIER

Progress in Organic Coatings 26 (1995) 1–28

PROGRESS IN ORGANIC COATINGS

Review Paper

Application of electrochemical impedance spectroscopy to study the degradation of polymer-coated metals

A. Amirudin, D. Thierry *

Swedish Corrosion Institute, Roslagsvägen 101 Hus 25, S-104 05 Stockholm, Sweden

Received 5 May 1995; revised 30 May 1995

Abstract

The recent widespread application of electrochemical impedance spectroscopy (EIS) to study the degradation of polymer-coated metals has been reviewed. The availability of modern instrumentation to obtain impedance data as well as computer programs to interpret the results have made the technique popular. In addition, EIS is very suited to the study of polymer-coated metals. However, despite, and even because of sophisticated methods of interpretation, some of the conclusions made in EIS studies remain questionable. A proliferation of equivalent circuits has been postulated without however confirmation by other experimental techniques. The significance and the reliability of different parameters obtained from EIS and used as criteria of coating deterioration remain controversial despite the large number of studies carried out. EIS has also been used, with limited success, to monitor in situ the degradation of polymer-coated metals in atmospheric exposure.

Keywords: Electrochemical impedance spectroscopy; Degradation; Polymer-coated metals

1. Contents

* Corresponding author.

SSDI 0300-9440(95)00581-X

2. Introduction

Corrosion, the destruction or deterioration of a material (or its properties) due to reaction with its environment, represents a tremendous economic loss and it has been estimated that the total annual cost of corrosion in the industrialized countries amounts to about 4% of the gross national product [1] or 2000–3000 dollars per inhabitant [2]. Of the several methods used to protect from corrosion, the use of coatings is the most popular method of protecting steel and other metals because it allows one to design a substrate with the desired physical and mechanical properties and to utilize a coating that is resistant to the environment to which the part is to be exposed, thus combining the best of two worlds [3]. Of the various types of protective coatings that are in use, organic polymer coatings predominate in protection against atmospheric corrosion of metals, and approximately 90% of all metal surfaces are covered with them [4]. The protection conferred by organic coatings is remarkable in view of the fact that they are so thin. Typically, a paint film is 25–50 μm thick [5], but some heavy-duty paints for ships may be as much as 250 μm thick [6], while protective lacquers on the inside of food cans are generally as thin as 5 μm [7]. Organic coating systems protect against metal corrosion by three mechanisms: the physicochemical (barrier), the electrochemical (inhibition or cathodic protection) and the adhesional mechanisms [8].

Paint coatings are tested for various purposes: to develop new coating materials; to determine the best coating for a particular environment; to control the quality of coatings; to study the fundamental properties of coatings and their mode of protection, etc. Paint tests may be physical (to test the primary properties of coatings), accelerated (by increasing the temperature and/or concentration of the corrosive species) atmospheric (with paints exposed at different geographical locations on earth) or electrochemical (as metals, even when painted, corrode electrochemically).

Of the electrochemical tests, the simplest to carry out is the measurement of the corrosion potential of the painted metal as a function of immersion time but its results are

difficult to interpret. The electrical resistance of the coating could give an indication of its efficiency as a barrier to ions [9,10]. Electrochemical resistance which is widely used to determine the corrosion rate of uncoated metal is not that much use for coated metals because the method used is valid only for activation controlled anodic metal dissolution reactions with the cathodic reaction either under complete activation control or the special case of complete diffusion control and in the absence of ohmic potential drops like that caused by the paint film. As the polarization is completely absorbed by the ohmic drop caused by the coating, the well known Stern–Geary relationship ($R_p = B/i_{corr}$) does not apply here [11]. Therefore, if meaningful results are to be obtained from this technique, a correction must be made for this potential drop. The anodic and cathodic polarization curve method has an additional disadvantage to the ohmic drop. It is not a non-destructive method as large excursions from the corrosion potential are likely to change conditions at the metal/paint interface so that the technique itself may cause defects in the paint [12].

A.c. methods have also been used to test coatings because when a polymer-coated metal is exposed to aqueous solutions, the measured capacitance of the coating increases with time due to the absorption of water by the coating [13]. A simple a.c. bridge was used to measure the capacitance. The method consists of applying a sinusoidal a.c. wave (of low voltage amplitude and a frequency of 1 kHz) to the polymer coated metal–electrolyte system and measuring the capacitance by a null method. This method also gives the a.c. resistance which is lower than the d.c. resistance [14]. Therefore, by the use of simple and inexpensive equipment, the ability of a coating to function as a barrier to water and ions may be determined by obtaining the capacitance and resistance of the coating, respectively.

A few other miscellaneous electrochemical methods have been described by Leidheiser [15]. However, reviewing the electrochemical methods used in assessing the corrosion of painted metals, Wolstenholme in 1973 concluded that "it was disappointing to note that the results of electrochemical tests so far performed have not been very informative" [16]. Since then, the widespread and successful application of electrochemical impedance spectroscopy (EIS) to study the degradation of polymer-coated metals has changed the situation.

The objective of this paper is to review the past work concerning the application of EIS to study the degradation of polymer-coated metals with particular emphasis on the significance of various parameters obtained from EIS and thus complementing a recent review which was more general [17].

3. Electrochemical impedance spectroscopy (EIS)

3.1. Fundamentals

The single-frequency a.c. method can supply only limited information on the mechanisms of paint degradation because true paint resistance and capacitance are frequency-dependent [18]. Electrochemical impedance spectroscopy (EIS) is the method in which the impedance of an electrochemical system is studied as a function of the frequency of an applied a.c. wave.

When a steady-state system is perturbed (say by an applied a.c. voltage) it relaxes to a new steady state. The time (in seconds) taken for this relaxation is known as the time constant, τ, and given by:

$$\tau = RC \tag{1}$$

where R is the resistance (in ohms) and C the capacitance (in farads) of the system. The analysis of this relaxation process would provide information about the system. The ratio of the response to the perturbation is the transfer function. When the applied perturbation is an a.c. potential and the response an a.c. current, the transfer function is the impedance. To simplify calculations further, the perturbation and response are transformed from a function of time into the frequency domain via a Laplace transformation. In the frequency domain, fast processes (with low τ) occur at high frequencies while slow processes (with high τ) occur at low frequencies. The frequency around which a process occurs may be ascertained by:

$$f = 1/2\pi\tau \tag{2}$$

Thus dipolar properties may be studied at high frequencies, bulk properties at intermediate frequencies and surface properties at low frequencies.

Impedance may also be considered as the 'resistance' to the flow of alternating current,

$$E = IZ \tag{3}$$

where E and I are waveform amplitudes for potential and current, respectively, and Z is the impedance. Two different components contribute to impedance. One is due to resistors and is known as the reactive or real component and represented by the letter a. The other arises from a.c. circuit elements such as capacitors, inductors etc. and is known as the reactive or imaginary component and represented by the letter b. Unlike the resistive impedance, the reactive impedance affects not only the magnitude of the a.c. wave but also its time-dependent characteristics (phase). For instance, when an alternating voltage wave is applied to a capacitor, the resulting current waveform will lead the applied voltage waveform by 90°. Due to this reason, it is convenient to introduce complex notation by incorporating the complex number j where

$$j^2 = -1 \tag{4}$$

Thus, if a system is perturbed by a sinusoidal potential varying with time t as

$$E(t) = E_0 \exp(j\omega t) \tag{5}$$

its response would be

$$I(t) = I_0 \exp(j\omega t - \theta) \tag{6}$$

provided it is linear. $E(t)$ and $I(t)$ are the instantaneous values and E^0 and I^0 the maximum values (peak amplitude) of the potential and current wave forms, respectively. θ is the phase angle difference and ω the angular frequency in radians given by

$$\omega = 2\pi f \tag{7}$$

where f is the frequency. Usually a low a.c. voltage of about 10 mV is applied to keep the system linear.

Introducing the complex notation enables the impedance relationships to be presented as Argand diagrams (Fig. 1) in both Cartesian (a, b) and polar coordinates (r and θ). The

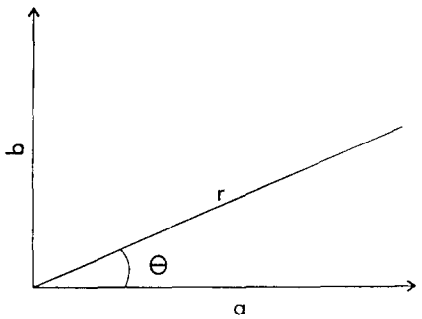

Fig. 1. Argand diagram showing impedance vectors.

former leads to the Nyquist impedance spectrum where the real impedance is plotted against the imaginary and the latter to the Bode spectrum where both r, the modulus of impedance, and the phase angle are plotted as a function of the frequency.

Mansfeld recommends the use of Bode plots for three reasons [19]: in Bode, all measured points are displayed equally while in Nyquist the majority of the points are located together at both ends of the spectrum; labelling of the curves in a Nyquist plot with frequency marks is quite cumbersome; and in Bode plots, R and C regions are clearly distinguished and together with the information provided by the frequency dependence of the phase angle, which is a very sensitive indicator of small changes in the spectra, a quick survey of the type of spectrum recorded is possible. However, most EIS spectra have been presented as Nyquist plots [20].

Irrespective of the way the results are presented, the equipment for EIS should obtain four parameters a, b, r and θ. These are computed from the raw data obtained which consists of the real and imaginary components of the voltage and current at each frequency applied.

3.2. *Instrumentation*

Almost all recent EIS investigations have used two kinds of instrumentation.

One is based on the single-sine technique in which a single frequency small amplitude sine wave signal is applied to the cell and the response measured. The frequency is then changed. Usually, the sweep begins from the higher to the lower frequencies in order to minimize sample perturbation. A frequency response analyzer (FRA) is used to generate the excitation waveform and analyze the response. An FRA is a digitally demodulated, stepped frequency impedance meter. It is also a digital correlation analyzer capable of measuring on two channels simultaneously. Thus an FRA determines the impedance of a test cell by correlating the cell's response with two synchronous reference signals, one in phase with the sine wave perturbation and the other phase shifted by 90°. A simplified schematic of a FRA is shown in Fig. 2.

The other type of instrumentation uses two techniques depending on the frequency range. At high frequencies (>5 Hz), the single-sine technique is used but with a lock-in amplifier to generate the excitation signal and analyze the response. A lock-in amplifier is a special type of a.c. voltmeter that uses phase sensitive detection circuitry to accurately measure the amplitude of a low signal obscured by background noise. At low frequencies,

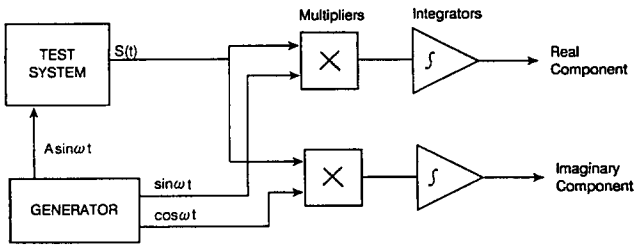

Fig. 2. Simplified schematic of a frequency response analyzer [25].

Table 1
Lock-in amplifier and FRA performance in an impedance system [25]

Lock-in	FRA
Advantages	
Very sensitive	faster analysis
Effectively removes background noise	wide frequency range
Minimizes harmonic distortion	removes harmonic distortion/d.c. components
Effectively suppresses d.c. noise	direct output to an external recording device
Relatively low cost	relatively easy stand-alone measurements
Disadvantages	
Limited frequency range	higher cost
Slower	limited background noise removal
Stand-alone measurements difficult	limited sensitivity

Table 2
Single-sine vs. multi-sine [25]

Single-sine	Multi-sine
Advantages	
High quality data	fast measurements
Fast high frequency measurements	mild perturbation
Simple instrumentation	improved signal-to-noise ratio
Wide bandwidth	more reliable plot
Disadvantages	
Slower low frequencies measurements	sensitive to harmonic distortion
Severe perturbation	vulnerable to aliasing

a multi-sine technique is used. This technique uses a fast Fourier transform (FFT) algorithm to process signals in the 50 μHz to 11 Hz range. The algorithm digitally generates a mixture of twenty excitation sine waves, each having different frequency and phase characteristics. The waveform (called pseudo-random white noise) is then applied to the test cell, producing a complex response waveform. The computer analyzes the response and extracts information at each of the discrete frequencies used to generate the excitation signal.

The merits and demerits of an FRA and a lock-in amplifier and that of the single-sine and multi-sine methods are given in Table 1 and Table 2, respectively.

Instrumentation is now available to cover a wide frequency range of 10^7 to 10^{-5} Hz [21] and usually 10 data points which are equally spaced on a logarithmic scale are measured

per decade of frequency. It is also possible to perform a sufficient number of measurements at each frequency in order to obtain satisfactory data and reduce the scatter of experimental data.

With any type of instrumentation, a potentiostat has to be used for potential control. It also provides a high input impedance to enable measurements to be made in systems with an impedance of up to 10^{10} ohms as even the best analyzers by themselves have an input impedance of only about 10^6 ohms. A third advantage of the potentiostat is that its series of current-measuring resistors eliminate the bandwidth problems that would be encountered by using the lock-in amplifier or FRA which have only one resistor. The current measuring resistor R_m should be such that [22]

$$10^{-2} > R_m/Z > 10^2 \tag{8}$$

One disadvantage of using a potentiostat in EIS is that it itself introduces a phase shift at high frequencies above 50 kHz [17]. Mansfeld et al. have recommended the use of a measuring resistor (corresponding to the electrolyte resistance between the Luggin capillary and the working electrode) at high frequencies to minimize this problem [23]. They also attribute the high-frequency phase shift to one more factor — the resistance and capacitance due to the fibre tip of the commercial reference electrode. Their solution to the latter problem is to place a Pt or Au wire either at the tip of the Luggin capillary or parallel to it (with its tip in the same plane as the capillary) and couple capacitively (with a 0.1 μF capacitor) parallel to the reference electrode [24].

The potentiostat can be dispensed with in some circumstances when measurements are made with only two electrodes. These circumstances are [25]: the two electrodes are of the same metal; one electrode is at least 10 times larger in area than the other; a power booster is used to handle high currents; or the measurement is to be made in a high impedance system such as a good coating which produces a low current.

3.3. *Validity*

A critical problem in impedance analysis is the validation of the experimental data. It is not uncommon to observe negative resistance (second quadrant) behaviour and inductive (fourth quadrant) behaviour when the experimental impedance data are presented as Nyquist plots. By merely inspecting the experimental data, it is not possible to ascertain whether or not the data are valid or have been distorted by some experimental artifact. Invalid impedance data may even yield seemingly correct kinetic parameters.

Macdonald et al. suggest the use of Kramers–Kronig (K-K) transforms to validate impedance data [26,27]. These transforms are a set of mathematical relations which transform the real component into the imaginary component and vice versa. The transfer function defining the relationship between a voltage perturbation and current response is impedance only when the following criteria are fulfilled.

(i) *Causality*. The response of the system is due only to the perturbation applied and does not contain significant components from spurious sources.

(ii) *Linearity*. The perturbation/response of the system is described by a set of differential laws. Practically, this condition requires that the impedance is independent of the magnitude of the perturbation.

(iii) *Stability*. The system must be stable in the sense that it returns to its original state after the perturbation is removed.

(iv) *Finity*. The transfer function must be finite valued at $\omega \rightarrow 0$ and $\omega \rightarrow \infty$ and must be a continuous and finite-valued function at all intermediate frequencies.

Under these conditions, a set of transforms between the real and imaginary components were shown to hold by Kramers [28] and Kronig [29]. That is, when the experimentally observed real component is transformed by K-K transforms, it should yield the experimentally observed imaginary component and vice versa. If it does not, then it cannot be interpreted as impedance [30].

However, Shih and Mansfeld [31,32] have questioned the use of K-K transforms to validate impedance data on the grounds that the condition of finity cannot be satisfied in many practical situations. They have pointed out that K-K transforms agree with experimental or theoretical data only in those cases where these data approach a d.c. limit within the frequency range used for the K-K transforms. In real systems, due to experimental problems, it is not possible to go down to frequencies as low as 10^{-6} Hz in order to approach this limit. Thus there is a possibility of valid impedance data being rejected because they do not transform according to K-K transforms. Other workers have also admitted that this problem exists in real systems [33].

3.4. Interpretation

Interpretation of EIS measurements is usually done by fitting the impedance data to an equivalent electrical circuit which is representative of the physical processes taking place in the system under investigation. In fact, one of the advantages of EIS is that impedance functions frequently display many of the features exhibited by passive electrical circuits. This is not surprising as the fundamental laws which connect charge and potential and which define the properties of linear systems are unchanged in passing from electronic to ionic materials. However, electrochemical interfaces being active (i.e. they generate noise independent of the input) rather than passive, and the elementary processes that are responsible for charge transfer being chemical rather than physical, sometimes an analogy is not possible. For example, impedance data in the second and third quadrant of the Nyquist plot imply a 'negative resistance' and cannot be represented by a classical equivalent circuit composed of passive elements. Therefore, it has been proposed that, in the first instance, impedance data should be interpreted in terms of reaction mechanisms rather than equivalent circuits [34].

The major problem in using equivalent circuits is to decide which specific equivalent circuit out of an infinite number of possibilities should be chosen. An equivalent circuit involving three or more circuit elements can often be rearranged in various ways and still yield exactly the same impedance. For example, the three circuits in Fig. 3 can have the same impedance at all frequencies when the parameters of the circuit are properly interrelated [35].

The most important elements that can be used in equivalent circuits are summarized in Table 3. The resistor, R, represents the resistor that charge carriers encounter in a specific process or material. The capacitor, C, represents the accumulation of charged species. The inductance, L, is used to represent the deposition of surface layers such as the passive layer.

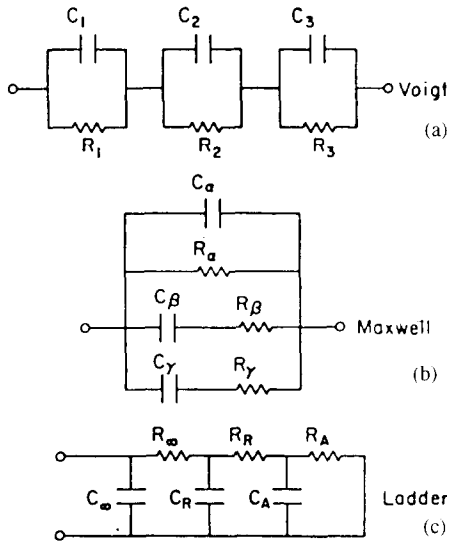

Fig. 3. Three circuits which can have the same impedance at all frequencies when the parameters of the circuit are properly interrelated [35].

The Warburg element, W, is used to model linear semi-infinite diffusion which occurs when the diffusion layer has infinite thickness. The constant phase element, CPE, is a general element which can represent a variety of elements such as inductance ($n=-1$), resistance ($n=0$), Warburg ($n=0.5$), capacitance ($n=1$) or non-ideal dielectric behaviour ($-1 \leq n \leq 1$) resulting from a distribution of relaxation times [36] or from non-uniform diffusion whose electrical analog is an inhomogeneously distributed RC transmission line [37]. The open boundary finite length diffusion, O, occurs when the diffusion layer has finite dimensions and one boundary imposes a fixed concentration for the diffusing species as in the case of oxygen conducting electrodes and corrosion related diffusion. The blocked finite length diffusion, T, occurs when the diffusion layer has finite dimensions and one boundary blocks the diffusing species as in the case of (thin) mixed conducting electrode. Other parameters in Table 3 are: Y_0, the frequency independent admittance; n, the power of the CPE; B, the diffusion factor given by

$$B = \delta/\sqrt{D} \tag{9}$$

Table 3
Electrical impedance elements

Element	Symbol	Impedance expression
Resistance	R	R
Capacitance	C	$1/(j\omega C)$
Inductance	L	$j\omega L$
Warburg	W	$1/[Y_0(j\omega)^{1/2}]$
CPE	Q	$1/[Y_0(j\omega)^n]$
OFLD	O	$\tanh[\{B(j\omega)^{1/2}\}/\{Y_0(j\omega)^{1/2}\}]$
BFLD	T	$\coth[\{B(j\omega)^{1/2}\}/\{Y_0(j\omega)^{1/2}\}]$

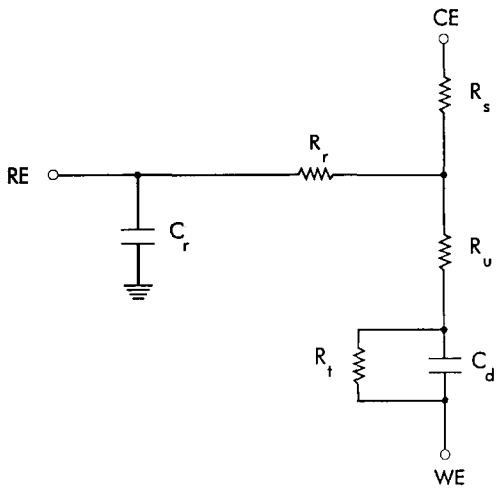

Fig. 4. Equivalent circuit for an electrochemical cell.

where δ is the Nernst diffusion layer thickness.

The equivalent circuit of a three-electrode electrochemical cell is shown in Fig. 4 where WE, CE and RE represent the working, counter and reference electrodes, respectively. R_s is the solution resistance, R_u is the uncompensated resistance, R_t is the charge-transfer resistance, R_r is the resistance of the reference electrode, C_d is the electrode double-layer capacitance and C_r is the parasitic loss to the ground in the leads.

Various methods have been used to select the correct equivalent circuit and to obtain the values of the elements in the circuit. Circuits with one time constant present no problem as the circuit and the values of the elements can be easily obtained graphically either from the Bode plot, or more commonly, from the Nyquist plot. For instance, the semi-circle shown in Fig. 5(b) may indicate the presence of only one time constant with the circuit consisting of a resistor and capacitor in parallel. The value of the resistance is given by the diameter of the circle in the real axis and the value of the capacitance is given by

$$C = 1/2\pi R f_{b\max} \tag{10}$$

where $f_{b\max}$ is the frequency (Hz) at which b is maximum. A similar analysis can be done if there are two time constants and the resulting semi-circles are well separated in the Nyquist plot. However, for the latter to happen, both the following criteria should hold [38],

$$\tau_1/\tau_2 > 20 \tag{11}$$

$$0.2 < (R_1/R_2) < 5 \tag{12}$$

which is not always the case and therefore the simple graphical method is of limited applicability.

Deconvolution of impedance data was one method that was used to interpret complex EIS spectra [39] but the sequence of extrapolations and subtractions tends to accumulate

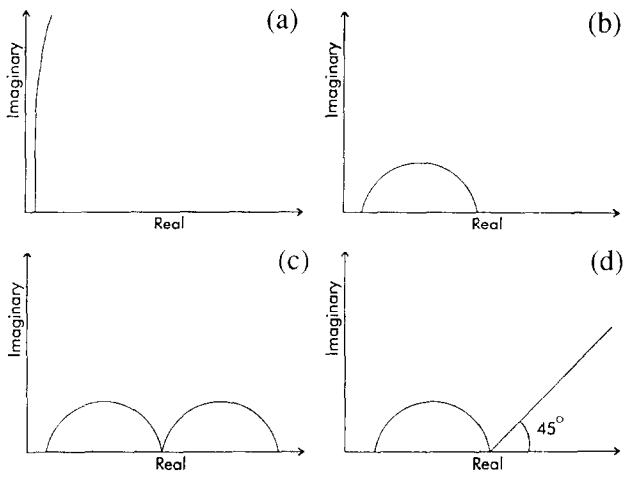

Fig. 5. Typical spectra: (a) capacitive behaviour; (b) one semi-circle; (c) two semi-circles; (d) 45° to real axis.

errors in the last-determined components and the method yields no estimate of curve fitting uncertainties [40].

The complex non-linear least-squares method (CNLLS) is more powerful and accurate than the graphical and deconvolution methods. This method uses all the experimental data (resistive and reactive components of impedance over a wide frequency range) simultaneously to fit a predetermined model to the data. Values of parameters of the model are determined by the analysis method such that errors between fitted data and experimental data are minimized.

Kendig et al. combined deconvolution with the CNLLS method in their CIRFIT program which minimizes the sum of squares of the radial difference between the observed and calculated impedance data presented in either the complex impedance or admittance plane [41]. This program provides estimates for the goodness-of-fit but can be applied only when there is observable separation of the time constants. Zeller and Savinell [42] modified CIRFIT to present ACFIT which however still uses only one equivalent circuit.

Many circuits can be used in the two most popular computer programs based on the CNLLS method, one developed by Macdonald et al. [43] and the other by Boukamp [44]. The Macdonald program has a variety of equivalent circuit models that can be chosen, arbitrary or analytical weighting and also a built-in procedure for avoiding or recognizing local minima in the sum-of-squares of fitting errors to be minimized. In the Boukamp program, the parameters of an equivalent circuit can be built arbitrarily by the operator and therefore elements can be added or subtracted from a conventional circuit. It also includes a program for the K-K transforms.

Schwiderke and Di Sarli [45] have proposed a non-iterative method based on a linear least-squares method for the study of organic coatings on metal substrates. As this method uses a linear least-squares method, it does not require initial guess values and therefore uses less processing time than the CNLLS method. Though it is faster, it is also less accurate. Walter et al. have used this method as basis of their ZCALC program which they have compared with the Macdonald and Boukamp programs [46].

It has recently been claimed that a straightforward circular regression method is better than the CNLLS method as it rapidly extracts the relevant parameters from the impedance spectra [47].

4. Application of EIS to organic coatings

4.1. Advantages

EIS is particularly suitable for the investigation of corrosion protection by organic coatings for the following reasons: it obtains a more complete view of the process of the deterioration of the paint coating and is able to distinguish effects that are either concealed or masked in other tests; it obtains precise quantitative data regarding the behaviour of the coatings, given that the data obtained with some of the other tests are rather subjective; it is a faster method for classifying and homologating the protective paint coatings.

4.2. Limitations

However, there are a few limitations in the use of EIS to study polymer-coated metals.

Firstly, it is quite impossible to derive a complete transfer function from fundamental knowledge of reaction mechanisms because of the overlapping of time constants. Most of the parameters describing the various processes are interdependent invalidating this kind of analysis. Therefore, equivalent circuits have to be used to interpret the EIS spectra which leads to another problem. Which of the multitude of equivalent circuits, all giving equally good fit with experimental data, should be chosen? This decision should be made only with a knowledge of the processes that occur and with the help of one or more independent techniques. For instance, Amirudin et al. have validated their proposed equivalent circuits by comparing the area of delamination obtained from EIS with that obtained from an image analyzer [48] and an IR thermographic method [49]. But this is not universally done. Though EIS is a powerful tool for the study of coated metals, it is not as yet a stand-alone method.

Another drawback is the poor reproducibility of data with a variation in magnitude of up to three orders of magnitude between replicate measurements due to the heterogeneity of the coating. One scheme for coping with such statistical error is to use five or more replicate measurements and scattergrams [50].

The Nyquist spectra of polymer-coated metals almost always display depressed semi-circles (i.e. their centres lie below the real axis). Depressed semi-circles often appear even in the case of uncoated metals and this phenomenon, referred to as impedance dispersion, is explained by the distribution of the time constants of the electrode process around a central value due to the roughness of the electrode surface [51,52] and/or the non-uniform distribution of the current density of the surface [53,54]. The depression of semi-circles in the Nyquist plots of polymer-coated metals is probably due to surface heterogeneity [55] or solid corrosion products of the metal substrate developing in the defects in the organic coating [56]. The latter explanation is supported by the observation that an intact (protective) coating shows no depression at all and the depression increases with the increasing

deterioration of the coating. Depressed Nyquist semi-circles are better represented by substituting CPE in place of capacitance [57].

Another limitation is that EIS cannot distinguish between the various coats applied on the substrate such as primer, topcoat etc. [58].

4.3. Special experimental requirements

A range of coating thicknesses — from as low as 4 μm [59] to as thick as 4000 μm [60] — have been studied by EIS. However, as polymer-coated metals have high impedance, the measurement of which may be beyond the capacity of the instrumentation used, the exposed area of the electrode needs to be increased with increasing coating thickness. For typical coatings,

$$\text{Area}(\text{cm}^2) > 0.4d \tag{13}$$

where d is the thickness of the paint in μm [61]. The above relationship is not relevant when there are defects in the coating such as voids, holidays etc. when a smaller area can be used.

Since a polymer-coated metal can be considered as a linear system — at least as long as it does not contain considerable corrosion damage — it is possible to use a larger a.c. signal than for bare metals and thereby decrease the scatter of the experimental data. A satisfactory approach involves the application of a.c. signals of about 100 mV in the high frequency range which are then decreased in the low frequency range [62]. By the same token, it is possible to use a higher amplitude at the beginning of the exposure when the coating is protective but reduce the amplitude when the coating begins to deteriorate.

4.4. Typical spectra

Impedance spectra of painted metals are characterized by different spectra depending on the state of the paint coating. Protective and intact coatings display a capacitive arc in the Nyquist plot (Fig. 5(a)). When the electrolyte penetrates the coating, the arc becomes a semi-circle (Fig. 5(b)). At later stages, the spectrum is characterized by more than one semi-circle (Fig. 5(c)) and sometimes a line inclined exactly at 45° to the real axis (Fig. 5(d)).

If the spectrum displays more than one semi-circle, usually it is the high-frequency semi-circle which contains paint information while the low-frequency semi-circle contains information about the processes related to reactions on the electrode surface [58,63]. However, Feliu et al. have pointed out three instances of this assumption not being valid [64]: paint coatings after a long exposure time [65]; artificially perforated films with the perforation recently formed; zinc-rich paint coatings during the first few days of exposure. In the first two instances, the low value of R_c would reduce the relaxation time, τ, to a magnitude so that the semi-circle attributed to it would appear at a frequency beyond the highest applied frequency and thus not be observed in the spectrum. In the case of zinc-rich paints, the arc obtained at higher frequencies is related to the response of a porous zinc electrode as at the beginning of the exposure the paint coating can act as a bare metal

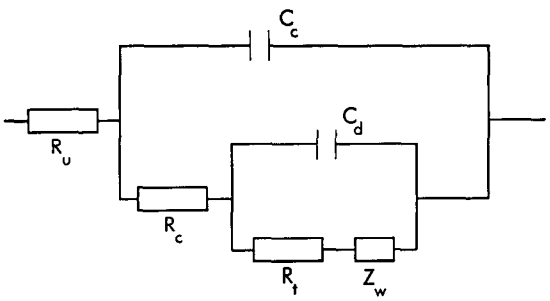

Fig. 6. General equivalent circuit for a polymer-coated metal.

because the zinc particles are in electric contact with each other and with the steel base up to the external surface of the coating.

When only one semi-circle is observed in the Nyquist plot, a simple method to identify whether it is due to the coating or due to the electrode reactions, is by varying the applied a.c. voltage [66]. A higher voltage should decrease the time constant due to the electrode reaction but should not normally affect the time constant due to the coating unless the pores are plugged by the higher voltage in which case it would increase.

4.5. *Equivalent circuits*

For a long time, the degradation of polymer-coated metals was represented by the general hierarchical circuit shown in Fig. 6 where R_u is the uncompensated solution/electrolyte resistance, R_c is the coating pore resistance, C_c is the coating capacitance, C_d is the electrode double-layer capacitance, R_t is the Faradaic charge-transfer resistance and Z_w is the Warburg diffusional impedance. Some have used this circuit as it is, while others have left out Z_w.

However, there is an increasing trend to present novel equivalent circuits. Cavalcanti et al. have proposed a circuit in which the coating and the faradaic impedances are connected in a series combination instead of the usual hierarchical one [67]. Circuits that include inductive elements have also been proposed [68,69]. Constant phase elements are being increasingly used in place of C_c and C_d because of the depressed semi-circles [70–72]. The mathematical relationship between a capacitance and the CPE is given by [73]:

$$C = Y_0 \omega^{n-1} / \sin(n\pi/2) \tag{14}$$

Amirudin and Thierry split up the charge-transfer resistance and the mass-transfer impedance of the electrode reaction into separate anodic and cathodic branches [48] which is in accord with a circuit resulting from a transmission line model for damaged automotive paint films [74]. van Westing et al. introduced an additional resistance associated with the diffusion process [75].

There is also an increasing tendency to split up the time constant due to the coating into separate time constants for the intact paint film and the delaminated paint pores [75–78].

A drawback in some of the novel circuits proposed is that the physical significance of some new passive elements included in the circuits is not explained. For instance, a time

constant in series with the electrode double layer proposed by two different groups of workers [79,80] remains unexplained. Another weakness of these new circuits is that they are not confirmed by other experimental techniques.

Recently, de Wit has shown the fallacy of correlating the number of time constants with the number of semi-circles appearing in the Nyquist plot [72]. Using the Boukamp program, the most probable impedance (MPI) circuit he derives contains four time constants for a spectrum containing only two visible semi-circles. Amirudin et al. confirm this observation [81]. Most probably, even the single semi-circle which is attributed either to the coating or to the Faradaic process may be found to be due to both if analyzed by the MPI method.

5. The significance of the passive elements

5.1. Uncompensated resistance, R_u

R_u is the uncompensated resistance between the reference electrode and the working electrode. It is also referred to as solution/electrolyte resistance. Scantlebury and Sussex attributed it to the resistance of the electrolyte solution as it decreases uniformly as the solution conductance is increased and as its actual values agree well with the resistance calculated for the solutions used [82]. However, according to Rowlands and Chuter, it is effectively a measure of the ionic film resistance as the actual solution resistance in electrolytes such as seawater is negligible [83]. This concept is supported by the observation that R_u values are generally higher for coated than uncoated metal in the same electrolyte [59]. Walter explained the high value obtained by him as due to stray capacitances [38].

Only in the case of very thin coats has R_u been used as a parameter of coating degradation and it was found to decrease with increasing degradation [59].

5.2. Coating capacitance, C_c

The coating capacitance C_c is given by:

$$C_c = \epsilon\epsilon_0 A/d \tag{15}$$

where ϵ is the dielectric constant of the coating, ϵ_0 is the permittivity of vacuum (i.e. 8.86×10^{-14} F/cm), A is the area of the coating and d is its thickness. As the dielectric constants of most coatings are in the range 3–4, the entry of water ($\epsilon=80$) into the coating should increase C_c as indicated earlier. Therefore, in the first instance, C_c should be a measure of water permeation into the coating.

A simple method of calculating the amount of water absorbed by the coating from the capacitance data is by using the empirical formula derived by Brasher and Kingsbury [13]:

$$X_v = \log(C_c/C_0)/\log 80 \tag{16}$$

where X_v is the volume fraction of water absorbed by the coating, C_0 is the coating capacitance at the beginning of exposure and 80 is the dielectric constant of water. From the

volume fraction, it is possible to determine the diffusion coefficient of water from computer programs [48,84,85].

Padget and Moreland found that in 3% NaCl solution, the rate of capacitance increase was in the order acrylic > alkyd > chlorine containing vinyl acrylic > chlorinated rubber [86]. The rate also depends on the surface pretreatment of the metallic substrate prior to painting, with the most effective treatments providing for the slowest increase [87].

According to Feliu et al., the advantage of using C_c as a parameter of coating behaviour is that it can be determined throughout the entire exposure period as it depends on deterioration on a microscopic scale along numerous points of the coating [87]. It also has the best reproducibility of all passive elements [88]. The disadvantage is that it gives indication of neither the deterioration of the paint nor the corrosion rate of the underlying metal but only on the water permeability, which could give, at the best, only an indirect information of the state of the coating and the risk of corrosion. Walter also confirms that C_c cannot be used as a parameter for coating degradation because it reaches a steady-state value after some time while the degradation of the coating continues [89]. He explains the relatively constant C_c value as follows: the capacitance of the small pathways being much less than the parallel capacitance of the remainder of the film, it does not contribute significantly to the overall capacitance even though the pathways controlled the performance of the paint film [58]. Scully also found that C_c cannot be correlated with coating deterioration of epoxy-polyamide-coated steel systems exposed to seawater [90]. However, he noticed that C_c continued to increase after hundreds of days of exposure and attributed this to a gradual increase in water solubility of the film due to its deterioration. It has also been reported that when Warburg behaviour was observed, delamination occurred when $d[C_c]/dt$ was greater than zero [91].

de Wit interpreted four regimes in the increase of C_c with time [72]. He also found that despite full saturation, no constant value for C_c was obtained due to swelling and therefore the coating was not behaving as an ideal dielectric [92]. Therefore it is better to replace C_c with a CPE and in such a case the admittance Y_0 continuously increases for several days [70] and is no longer a parameter of water absorption but instead indicates delamination [72]. In fact, the factor n of the CPE has been used as a parameter to monitor coating degradation [93,94].

The use of a capacitance instead of a CPE also leads to authors reporting very high water uptake (9–25%) by the coating [95–97].

A few workers have found that C_c decreases initially before increasing [98,99] and attributes this to one or more of the following reasons: the water is not randomly distributed in the polymer coating; additional internal stresses in the coating created by water uptake and swelling lower the dielectric permittivity; the adsorption or reaction of water may change the dielectric behaviour of the coating.

In summary, C_c seems to be a measure of water absorption only at the initial stage of exposure and when the coating has been exposed for days C_c reflects coating delamination and degradation [85].

5.3. *Coating resistance, R_c*

R_c has been generally interpreted [38,100–102] as the pore resistance of the coating resulting from the penetration of the electrolyte. Electrolyte penetration may occur through

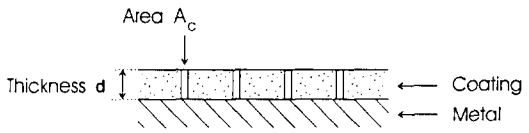

Fig. 7. Schematic representation of a paint film traversed by capillary channels.

real (microscopic) pores and/or virtual pores defined by regions in the polymer of low crosslinking and therefore high transport [103,104].

R_c can be related to the number of pores or capillary channels perpendicular to the substrate surface through which the electrolyte reaches the interface as follows:

$$R_c = d/\kappa N A_c \tag{17}$$

where κ is the conductivity of the electrolyte, N is the number of channels, A_c is the average cross-sectional area of the channels and d is the length of the channels which is equal to the coating thickness (Fig. 7). The resistance of the layer of electrolyte which would occupy the same space (and hence the same thickness) as the coating can be calculated from the formula:

$$R_e = d/\kappa A \tag{18}$$

where A is the total area of the coated metal. Combination of Eqs. (17) and (18) yields:

$$R_e/R_c = NA_c/A \tag{19}$$

The fraction NA_c/A may be termed as the porosity of the coating. Armstrong and Wright found that the porosity of the coating thus calculated is about 10^5 times lower than the delaminated area under the coating which made them to conclude that though the electrolyte reaches the interface through few pores, it causes rapid delamination by spreading along the interface [105]. This delamination may be due to the corrosion of the metal causing undercutting of the coating or, possibly, the poor adhesion of the film to the surface [106]. Thermogravimetric analysis in combination with EIS has shown that the mean pore area is greater at upper layers and smaller at layers inside the coating and a mean pore should have dimensions as presented in Fig. 8 [107].

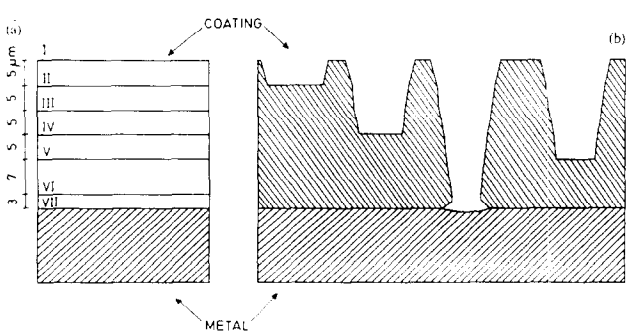

Fig. 8. Schematic representation of different layers of the coating (a) and model of conducting macropores through the coating as a consequence of electrolyte penetration (b) [107].

Thus the magnitude of R_c at a given time is indicative of the state of degradation of the paint film caused by solution ingress via pathways through the film [58,102]. A coating resistance of 10^6 ohm cm^2 is generally viewed as being indicative of a good organic coating [108]. Scully and Hensley have pointed out that this threshold value is valid only for steel substrate and not for magnesium substrate [108]. In addition to being substrate-specific, the threshold value is also electrolyte-specific because the magnitude of R_c depends mainly on the conductivity of the penetrating electrolyte (Eq. (17)). Indeed, this has been observed [95] and Amirudin and Thierry have reported a linear relationship between R_c and the conductivity of NaCl solutions of different concentrations [49].

As ionic penetration is slower than water penetration, unlike C_c, R_c cannot be determined at early periods of exposure and is also not reproducible at advanced deterioration because of the formation of macroscopic and random perforations [88]. In fact, variation of one or two orders of magnitude between replicates has been observed [109].

Though R_c can also increase with time probably as a result of pore or defect blockage by corrosion products [71,110] it usually decreases. For a given polymer coating, the coating/metal interface most susceptible to corrosion will induce the most rapid decrease in R_c [102]. R_c for a free film remains essentially constant and therefore the presence of the substrate enhances the short circuiting of the polymer film by the conducting electrolyte.

Quite a few workers [89,102,104,111] have found three regions in the time-dependent decrease of R_c. It initially decreases rapidly, then slowly (exhibiting a plateau) and then again rapidly coinciding with the appearance of the second semi-circle. Walter explains the plateau by making the assumption that the number of pathways forming is approximately constant with time [89]. While one additional pathway will cause a relatively large decrease in R_c when a small number of pathways exist, it will cause only a small decrease when a large number of pathways exist. However, Touhasent and Leidheiser attribute the first two regions to different ways of electrolyte permeation, the first sharp fall resulting from the penetration of the electrolyte into microscopic pores and the second fall resulting from the penetration of the electrolyte into the virtual pores of the polymer matrix [112]. Though R_c has always been associated with electrolyte penetration, Miskovic-Stankovic et al. are the first to attribute it to water penetration and they argue that the first region of the curve corresponds to the saturation of the coating with water and the second region to the penetration of water and electrolyte through macropores [107]. All agree that the third region is due to delamination and corrosion.

Indeed, Haruyama et al. identify the change in R_c only with delamination [113]. According to them, R_c is the resistance of the coating which is infinite before the electrolyte reaches the interface. With the arrival of the electrolyte, a double layer forms at the disbonded region of the coating/metal interface and corrosion begins giving finite values for R_c. Therefore, R_c is a measure of the disbonded area A_d:

$$R_c = R_c^0 / A_d \tag{20}$$

where

$$R_c^0 = \rho d \tag{21}$$

ρ being the specific bulk resistivity and d the thickness of the coating.

Mansfeld and Tsai do not find anything wrong in Haruyama's assumption that current flow will occur only in those areas, A_d, where coating delamination has occurred [114]. However, Kendig et al. cast doubt on the Haruyama assumption on the basis of experiments conducted with free films [115]. The results of Armstrong et al. described above [105,106] also refute the concept advocated by Haruyama et al.

5.4. Double-layer capacitance, C_d

C_d is usually at least one order of magnitude higher than C_c [89] and unlike in the case of C_c and R_c, there is unanimity of opinion in the interpretation of C_d. Almost all agree that it is a measure of the area over which the coating has disbonded [20,87,105]. The area of delamination may be calculated from the formula

$$A_d = C_d / C_d^0 \tag{22}$$

where $C_d{}^0$ is the area-specific double-layer capacitance of the uncoated metal.

However, while studying mild steel and galvanized steel substrates coated with paints containing passivating pigments, Amirudin and Thierry observed that C_d is more a measure of the electroactive area than the delaminated area [48]. Thus C_d may also depend on the electrochemical state of the surface (i.e. active or passive). The disadvantage of using C_d as an indication of coating degradation is that it can be measured only at advanced stages of coating deterioration when the EIS spectrum indicates at least two time constants.

5.5. Charge-transfer resistance, R_t

In theory, the value of R_t would be the most appropriate parameter for monitoring the protective properties of the coating as the corrosion rate of the underlying metal can be estimated from the Stern–Geary equation, but again, like C_d, R_t can be estimated only when at least two time constants are evident in the spectrum. Unlike in uncoated metal, R_t decreases with time [116] and, therefore (like C_d) R_t also depends in the first instance on the area of coating delamination according to [95,105,117]:

$$A_d = R_t^0 / R_t \tag{23}$$

where $R_t{}^0$ is the area-specific charge-transfer resistance of the uncoated metal.

Sometimes, the ratio R_t/R_c is constant over a period of time in which case it is concluded that substrate corrosion is due to ionic diffusion through the coating and not to delamination [89,118]. This conclusion about the relationship between corrosion and diffusion is supported by Mansfeld and co-workers who thought, conversely, that the corrosion reaction at the substrate/coating interface enhances the conduction at defects in the coating [101,102]. However, this conclusion will not be valid if Haruyama's interpretation of R_c is accepted as then both R_c and R_t depend on delamination and the ratio R_t/R_c will always remain constant.

5.6. Warburg impedance, Z_w

The Warburg impedance has received very little attention in publications dealing with EIS, which is surprising since it implies the possibility of measuring diffusion constants [100]. It can be also defined by:

$$Z_w = \sigma\omega^{-1/2}(1-j) \tag{24}$$

where σ, the Warburg coefficient, is related to Y_0 by:

$$\sigma = 1/Y_0\sqrt{2} \tag{25}$$

and to the diffusion coefficient of the species, D, by [119]:

$$\sigma = RT/\sqrt{2}n^2F^2cD^{1/2} \tag{26}$$

Warburg impedance is usually characterized by a 'diffusion tail' in the Nyquist plot which is inclined exactly at 45° to the real axis (Fig. 5(d)). The relative values of R_t and σ determine whether the system is charge-transfer controlled or diffusion controlled; in general, the system is under charge-transfer control for $R_t/\sigma > 10$ and under diffusion control if $R_t/\sigma < 0.1$ [120].

Eq. (24) assumes that the a.c. diffusion layer thickness (i.e. the distance travelled by the diffusing species in the low-frequency oscillating perturbations) is very much less than the d.c. Nernstian diffusion layer thickness [38]. When both a.c. and d.c. diffusion layer thicknesses are comparable, the diffusion tail may bend towards the real axis at low frequencies resulting in a skewed semi-circle and the diffusion is better expressed as the open boundary finite length diffusion (OFLD), in which case the diffusion impedance expression (Eq. (24)) becomes:

$$Z_d = \sigma\omega^{-1/2}(1-j)\ \tanh\{\delta(j\omega/D)^{1/2}\} \tag{27}$$

This has been done by Geenen et al. who have replaced the Warburg diffusion with OFLD in some equivalent circuits proposed by them [79].

The time constant for a diffusion process may be calculated from the equation [100]:

$$\tau = d^2/D \tag{28}$$

If an equivalent circuit contains only one diffusion element, it is usually attributed to the cathodic oxygen diffusion but Fastrup and Saarnak have proposed that this diffusion element is related to the anodic diffusion through corrosion products in the pores or larger holes [100].

6. Parameters from the Bode plot

In addition to the passive elements in the equivalent circuit, other parameters obtained from the Bode plot of the impedance spectrum have been used to monitor the state of polymer-coated metal. Fig. 9 shows these parameters and a brief description of each is given below in the order they appear when sweeping from high to low frequencies. It should be noted that the lower the frequency of interest, the harder it is to obtain the parameter as there is data scatter at the low frequency part of the spectrum especially if the coating is protective.

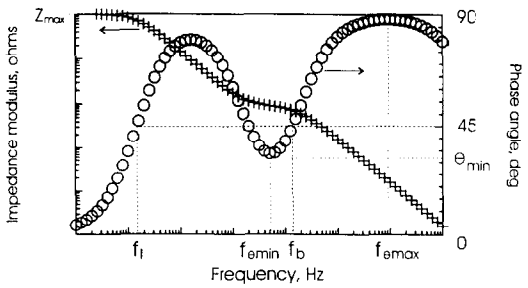

Fig. 9. Parameters obtained from the Bode plot and used for monitoring coating degradation.

6.1. *Frequency at maximum phase angle, $f_{\theta max}$*

Sekine et al. have used the frequency at which the phase angle is maximum, $f_{\theta max}$, to monitor coating performance [120]. They arrived at the theoretical relationship:

$$\log(f_{\theta max}) = -\log(2\pi) - 0.5\log(R_u C_c^2) - 0.5\log(R_c) \quad (29)$$

They observed a linear relationship between $f_{\theta max}$ and R_c and thus $f_{\theta max}$, which can be measured easily, could serve as a criterion of coating resistance.

6.2. *Breakpoint frequency, f_b*

On scanning the frequency from high to low values in EIS, the frequency at which the phase angle first falls to 45° is the breakpoint frequency, f_b. It was originally proposed by Haruyama et al. [113] and is a consequence of their assumption that coating resistance is a function of the delaminated area (Eq. (20)). They also followed the general assumption that C_c is the dielectric capacitance depending on the entire area of the coating:

$$C_c = C_c^0 A \quad (30)$$

where $C_c{}^0$ is the area-specific value and A is the total area of the specimen. When the phase angle is 45°, the resistive and reactive impedances are equal:

$$R_c = 1/2\pi f_b C_c \quad (31)$$

or

$$f_b = 1/2\pi R_c C_c \quad (32)$$

Substituting from Eqs. (20) and (30):

$$f_b = A_d/2\pi R_c^0 C_c^0 A \quad (33)$$

From Eq. (15)

$$C_c/A = C_c^0 = \epsilon\epsilon_0/d \quad (34)$$

On substituting for $R_c{}^0$ and $C_c{}^0$ from Eqs. (21) and (34), Eq. (33) becomes:

$$f_b = A_d/2A\pi\rho\epsilon\epsilon_0 \quad (35)$$

or

$$f_b = f_b^0 A_d / A \tag{36}$$

According to Eq. (36), the breakpoint frequency is a measure of the disbonded area provided the dielectric constant, ϵ, and the resistivity of the paint, ρ, remain constant. Another assumption implicit in the method is that the impedance is represented by the general equivalent circuit shown in Fig. 6.

However, the validity of the breakpoint frequency method (BFM) has been questioned by some. As described above, both Kendig et al. [115] and Armstrong et al. [105,106] refute Eq. (20) and therefore the BFM itself. According to van der Weijde et al., the hierarchical equivalent circuit chosen by Haruyama is incorrect [121]. They also point out that when many breakpoints are close together, it is not possible to distinguish between them. In fact, it has been mathematically shown that when the second time constant is close enough to the first so that the magnitude of C_d is comparable to C_c, the breakpoint frequency is not a measure of the area of delamination [122].

The assumption that the dielectric constant, ϵ, and the resistivity of the paint, ρ, remain constant, is also invalid. But as ϵ increases with the entry of water and ρ decreases with the entry of the electrolyte, the two variations must cancel each other if BPM is to be valid. This is not so. In fact, Murray and Hack have used the difference in the variation in ϵ and ρ in the initial period of exposure to determine coating behaviour [123]. As water penetrates the coating before the ions, first ϵ increases leading to a decrease in f_b as per Eq. (35). When the ions penetrate later, ρ decreases leading to an increase in f_b as per Eq. (35). Thus, if the coating disbonding is limited by ionic transport processes, then the minimum in the initial breakpoint frequency values may be a useful parameter to compare different paints.

The surprising thing about BPM is that despite such a number of flaws, many workers have found good correlation between the breakpoint frequency and the delaminated area determined by an independent technique [90,124]. Amirudin et al. have found the breakpoint frequency to be a reliable indicator of delamination in various environments — total immersion [49], cyclic corrosion tests [125] and even atmospheric exposure [80].

6.3. *Minimum phase angle, θ_{min}, and its frequency, $f_{\theta min}$*

As ϵ increases due to water uptake and ρ decreases as conductive paths and defects develop in the coating, $f_b{}^0$ in Eq. (36) is not a constant value. This led Mansfeld and Tsai to propose two additional parameters, the minimum phase angle θ_{min}, and its frequency, $f_{\theta min}$, as indicators of coating delamination [114]. The analytical relationships between these parameters and the delaminated area are quite complicated. However, making certain simplifying assumptions it was shown that θ_{min} and the ratio $f_b/f_{\theta min}$ are both dependent only on the delaminated area and neither on ϵ nor ρ.

6.4. *Low breakpoint frequency, f_l*

As f_b gave a good correlation only in the case of marginal and poor coatings where the disbonded area was 1–75%, Murray and Hack [126] have successfully used the low breakpoint frequency, f_l, proposed by Hack and Scully [127] to detect disbonded areas as

low as 0.01%. The low frequency f_1 is related to the second time constant and is the frequency at which the reactive impedance due to the double layer is equal to the sum of the charge-transfer and coating resistances:

$$R_t + R_c = 1/2\pi f_1 C_d \quad (37)$$

By proceeding as in the case of f_b, a mathematical expression may be derived according to which f_1 is dependent on defect area for very small defects where f_b is not resolvable.

6.5. *Maximum impedance, Z_{max}*

Murray and Hack [128] used several parameters to monitor coating performance and found the maximum impedance at low frequency, Z_{max}, to be the most useful parameter thus confirming the original claims made by Bacon et al. 45 years ago [9] on the usefulness of d.c. resistance values to characterize organic coatings. Others too are of the same opinion [129].

7. Using EIS to monitor atmospheric corrosion

Almost all EIS investigations of polymer coatings have been made in aqueous environments and hence the results may not be correlated to service in atmospheric conditions. Even if samples are exposed to atmospheric conditions, their impedance spectra are obtained by using an extraneous electrolyte [130]. Walter has found that though this procedure does determine relative performance of different paints exposed to the same conditions, the absolute value of R_c depends on the conductivity of the solution used for the measurement [95]. The time of immersion in the electrolyte before measurements are done is also critical and it has been reported that six hours were optimum to get a clear correlation between visual and impedance studies [71].

Simpson et al. developed an atmospheric electrochemical monitor (ATMEIS) to obtain EIS spectra in atmospheric conditions thus eliminating the need for an extraneous liquid electrolyte [131]. This monitor consisted of a painted steel coupon upon which a gold electrode (covering less than 10% of the surface of the sample coupon) is electron-beam deposited (to a thickness of 200 nm) to serve as both reference and counter electrode. The monitor relies on the assumption that as the gold electrode is placed at the surface of the coating, its entire area is wetted and utilized resulting in a low interfacial impedance relative to the coating or steel/coating interface. According to these workers, ATMEIS has been tested both in immersion exposure and in an atmospheric chamber and has been found to generate EIS data consistent with those predicted for a painted metal coupon in an aggressive environment [132–134].

Barreau and Thierry developed a sensor similar to ATMEIS but which differs from the latter mainly in the method of gold deposition [135]. They used a simpler one-step method, depositing gold on to the painted panel while it is covered with a shield so as to produce the required design. The gold layer thickness was also twice (400 nm) as much as that in the ATMEIS. The validity of the two-electrode configuration using gold as counter-cum-reference electrode has been tested by these workers who demonstrated that, under the

experimental conditions used the interfacial impedance of the gold electrode was negligible compared to the total impedance of the system.

Other workers have found that the deposition of gold on the paint does not affect coating parameters [136].

Amirudin et al. have used the sensor developed by Barreau and Thierry to study the degradation of epoxy-coated galvanized steel in various environments such as chloride [125], sulfur dioxide [137] and marine atmosphere [80]. They found the sensor to be an efficient tool to study in situ the deterioration of polymer-coated metal without the use of an extraneous electrolyte but realized that it would be reliable only when the conductivity of the moisture film covering the sensor is more-or-less constant (as in controlled laboratory tests) because the magnitude of the passive elements depends not only on delamination but also on this conductivity [49,138]. They also observed that, contrary to earlier claims, the impedance of the gold does modify the low frequency part of the spectrum, especially in largely delaminated low-impedance systems, and therefore the equivalent circuit should incorporate a time constant for the gold [49,138].

8. Concluding remarks

It is obvious from the preceding discussion that a tremendous amount of work has been done during the last twenty years in the application of EIS to study the performance of polymer-coated metals. The popularity of the EIS technique is due to two factors: its suitability to the study of polymer-coated metals and the availability of modern instrumentation (to obtain the spectra) and computer programs (to interpret it). This is why, though the impedance technique was known to the scientific world for several decades, the sudden upsurge has occurred only during the last couple of decades.

Though much insight has been now gained on the application of EIS to polymer-coated metals, very few controversies have been settled beyond doubt. These include the application of Kramers–Kronig transforms to validate the impedance data, the substitution of CPE instead of capacitance in the equivalent circuit, the significance of the coating resistance and the usefulness of the breakpoint frequency. The last two items are of critical importance because the coating resistance and the breakpoint frequency are becoming the most popular impedance parameters of coating delamination as both are obtainable in the early stages of deterioration. The maximum impedance, Z_{max} is also beginning to become popular.

One clear advantage of the technique is its ability to detect very minute areas of disbondment in situ. There is no other simple technique which could yield this vital information.

At the present time, the use of equivalent circuits seems to be indispensable for the interpretation of data. Though many novel equivalent circuits have been proposed, the physical significance of most of these circuits cannot be easily understood especially with respect to the line of current flow and very few of these circuits have been confirmed by another experimental technique. It is interesting to note that most of the novel circuits result from those who use the Boukamp program, which can yield any type of equivalent circuit. It has been recently suggested that the power of such software should not be overestimated and that the proposed equivalent circuit should fulfil three criteria [139]: it should be

physically meaningful; it should give a good fit with experimental data; it should be confirmed by one or two other techniques.

The atmospheric corrosion monitor had only a limited success. Initial reports were very encouraging but the realization that the magnitude of the passive elements depends not only on the area of delamination but also on the conductivity of the electrolyte film on the surface of the monitor, precludes its use in actual atmospheres. At best, the monitor can be used only in accelerated laboratory tests with simulated atmospheres.

It is hoped that the next decade will throw more light on the technique and confirm that EIS is indeed a powerful tool to study the degradation of polymer-coated metal.

References

[1] E. Mattsson, *Basic Corrosion Technology for Scientists and Engineers*, Ellis Horwood, Chichester, UK, 1989, p. 13.
[2] G. Wranglen, *An Introduction to Corrosion and Protection of Metals*, Chapman and Hall, London, 1985, p. xv.
[3] H. Leidheiser, Jr., in F. Mansfeld (ed.), *Corrosion Mechanisms*, Marcel Dekker, New York, 1987, p. 165.
[4] K. Barton, *Protection against Atmospheric Corrosion*, Wiley, New York, 1976, p. 106.
[5] W.M. Morgans, *Outlines of Paint Technology*, Vol. 2, Charles Griffen, USA, 2nd edn., 1984.
[6] T.A. Banfield, *Marine Finishes*, OCCA Monograph No 1, Oil and Colour Chemists Association, 1980.
[7] C.G. Demmer and N.S. Moss, *J. Oil Colour Chem. Assoc., 65* (1982) 249.
[8] W. Funke, in R.A. Dickie and F.L. Floyd (eds.), *Polymeric Materials for Corrosion Control*, American Chemical Society Symposium, USA, 1986, p. 222.
[9] R.C. Bacon, J.J. Smith and F.M. Rugg, *Ind. Eng. Chem., 40* (1948) 161.
[10] J.E.O. Mayne and D.J. Mills, *J. Oil. Colour Chem. Assoc., 58* (1975) 155.
[11] L.M. Callow, J.A. Richardson and J.L. Dawson, *Br. Corros. J., 11* (1976) 132.
[12] T.A. Strivens and C.C. Taylor, *Mater. Chem., 7* (1982) 199.
[13] D.M. Brasher and A.H. Kingsbury, *J. Appl. Chem., 4* (1954) 62.
[14] M. Buller, J.E.O. Mayne and D.J. Mills, *J. Oil. Colour Chem. Assoc., 59* (1976) 351.
[15] H. Leidheiser., *J. Coat. Technol., 63* (802) (1991) 21.
[16] J. Wolstenholme, *Corros. Sci., 13* (1973) 521.
[17] U. Rammelt and G. Reinhard, *Prog. Org. Coat., 21* (1992) 205.
[18] G.W. Walter, *Corros. Sci., 30* (1990) 617.
[19] F. Mansfeld, *Corrosion, 44* (1988) 558.
[20] G.W. Walter, *Corros. Sci., 26* (1986) 681.
[21] Solartron 1255 HF Frequency Response Analyzer, *User Manual*, UK.
[22] J.D. Scantlebury, K.N. Ho and D.A. Eden, in F. Mansfeld and U. Bertocci (eds.), *Electrochemical Corrosion Testing, ASTM STP 727*, American Society for Testing and Materials, 1981, p. 187.
[23] F. Mansfeld, S. Lin, Y.C. Chen and H. Shih, *J. Electrochem. Soc., 135* (1988) 906.
[24] F. Mansfeld, M.W. Kendig and T. Tsai, *Corrosion, 38* (1982) 570.
[25] *Application Note AC-3*, Princeton Applied Research, NJ, USA.
[26] D.D. Macdonald and M.U. Macdonald, *J. Electrochem. Soc., 132* (1985) 2316.
[27] M.U. Macdonald, S. Real and D.D. Macdonald, *J. Electrochem. Soc., 133* (1986) 2018.
[28] H.A. Kramers, *Phys. Z., 30* (1929) 521.
[29] R. de L.Kronig, *J. Opt. Soc. Am., 12* (1926) 547.
[30] B.D. Cahan and C.T. Chen, *J. Electrochem. Soc., 129* (1982) 474.
[31] H. Shih and F. Mansfeld, *Corros. Sci., 29* (1988) 933.
[32] H. Shih and F. Mansfeld, *Corrosion, 45* (1989) 325.
[33] P. Agarwal, M.E. Orazem and L.H. Gracio-Rubio, *J. Electrochem. Soc., 139* (1992) 1917.
[34] D.D. Macdonald, *Corrosion, 46* (1990) 229.

[35] J.R. Macdonald, *Impedance Spectroscopy*, Wiley, New York, 1987, p.96.
[36] J.R. Macdonald and M.K. Brachman, *Rev. Mod. Phys., 28* (1956) 393.
[37] J. Schrama, *Ph.D. Thesis*, University of Leiden, Netherlands, 1957.
[38] G.W. Walter, *J. Electroanal. Chem., 118* (1981) 259.
[39] R. Delevie, J.W. Thomas and K.M. Abbey, *J. Electroanal. Chem., 62* (1975) 111.
[40] R. Delevie and D. Vukadin, *J. Electroanal. Chem., 62* (1975) 95.
[41] M.W. Kendig, E.M. Meyer, G. Lindberg and F. Mansfeld, *Corros. Sci., 23* (1983) 1007.
[42] R.L. Zeller III and R.F. Savinell, *Corros. Sci., 26* (1986) 59.
[43] J.R. Macdonald, J. Schoonman and A.F. Lehnen, *J. Electroanal. Chem., 131* (1982) 77.
[44] B. Boukamp, *Proc. 9th European Corrosion Congr., Utrecht, Netherlands, 1989*, FU-252.
[45] E.E. Schwiderke and A.R. Di Sarli, *Bull. Electrochem., 3* (1987) 107.
[46] G.W. Walter, D.N. Nguyen and M.A.D. Madurasinghe, *Electrochim. Acta, 37* (1992) 245.
[47] T. Hamaide, G. Levallet and F. Henry., *Electrochim. Acta, 36* (1991) 1033.
[48] A. Amirudin and D. Thierry, *Br. Corros. J., 30* (1995) 128.
[49] A. Amirudin and D. Thierry, *Br. Corros. J., 30* (1995) 214.
[50] W.S. Tait, *J. Coat. Technol., 66* (834) (1994) 59.
[51] D.A. DeVooys and J.H.A. Pieper, *J. Electroanal. Chem., 72* (1976) 147.
[52] J.A. Harrison and P.J. Stronach, *J. Electroanal. Chem., 72* (1976) 239.
[53] I. Epelboin and M. Keddam, *J. Electrochem. Soc., 117* (1970) 1052.
[54] M. Nisancioglu and J. Newman, *J. Electrochem. Soc., 120* (1973) 1339.
[55] K. Hladky, L.M. Callow and J.L. Dawson, *Br. Corros. J., 15* (1980) 20.
[56] U. Rammelt, G. Reinhard and K. Rammelt, *J. Electroanal. Chem., 180* (1984) 327.
[57] D.C. Silverman and J.E. Carrico, *Corrosion, 44* (1988) 280.
[58] G.M. Walter, *Corros. Sci., 32* (1991) 1049.
[59] J.W. Nicholson, *Surf. Coat. Int. (J. Oil Colour Chem. Assoc.) 77* (1994) 472.
[60] M.J.L. Ostergard, A. Visgård and E. Maahn, *J. Oil Colour Chem. Assoc., 76* (1993) 29.
[61] M. Kendig and J. Scully, *Corrosion, 46* (1990) 22.
[62] F. Mansfeld, *Solartron Tech. Rep. No. 26*, Schlumberger Technologies, UK, 1993.
[63] U. Rammelt and G. Reinhard, *Prog. Org. Coat., 24* (1994) 309.
[64] S. Feliu, M. Morcillo and J.C. Galvan, in J.D. Scantlebury and M. Kendig (eds.)., *Proc. Symp. Advances in Corrosion Protection by Organic Coatings*, The Electrochemical Society, USA, 1989, p. 280.
[65] S. Feliu, J.C. Galvan and M. Morcillo, *Prog. Org. Coat., 17* (1989) 143.
[66] I. Thompson and D. Campbell, *Corros. Sci., 36* (1994) 187.
[67] E. Cavalcanti, O. Ferraz and A.R. Di Sarli, *Prog. Org. Coat., 23* (1993) 185.
[68] S. Narain, N. Bonanos and M.H. Hocking, *J. Oil Colour Chem. Assoc., 66* (1983) 48.
[69] J.A. Grandle and S.R. Taylor, *Corrosion, 50* (1994) 792.
[70] E. Frechete, C. Compere and E. Ghali, *Corros. Sci., 33* (1992) 1067.
[71] C. Compere, E. Frechete and E. Ghali, *Corros. Sci., 34* (1993) 1259.
[72] J.H.W. de Wit, in J.M. Costa and A.D. Mercer (eds.), *Progress in the Understanding and Prevention of Corrosion*, The Institute of Materials, London, UK, 1993, p. 240.
[73] E.P.M. van Westing, G.M. Ferrari and J.H. de Wit, *Corros. Sci., 34* (1993) 1511.
[74] C. Diaz, M. Urquidi-Macdonald, D.D. Macdonald, A.C. Ramamurthy, M.J. van Ooij, A. Sabata, M. Ström and G. Ström, *Proc. 12th Int. Corrosion Congr., Houston, TX, 1993*, Vol 5A, p. 3508.
[75] E.P.M. van Westing, G.M.Ferrari and J.H.W de Wit, *Corros. Sci., 36* (1994) 1323.
[76] J. Titz, G.H. Wagner, H. Spahn, M. Ebert, K. Juttner and W.J. Lorenz, *Corrosion, 46* (1990) 221.
[77] R. Hirayama and S. Haruyama, *Corrosion, 47* (1991) 952.
[78] S. Lin, H. Shih and F. Mansfeld, *Corros. Sci., 33* (1992) 1331.
[79] F.M. Geenen, J.H.W. de Wit and E.P.M. van Westing, *Prog. Org. Coat., 18* (1990) 299.
[80] A. Amirudin, C. Barreau, D. Massinon and D. Thierry, *Proc. 2nd Int. Conf. Zinc and Zinc Alloy Coated Steel Sheet, GALVATECH 92, Amsterdam, Netherlands, 1992*, p. 549.
[81] A. Amirudin, C. Barreau and D. Thierry, *Proc. 12th Int. Corrosion Congr., Houston, TX, 1993*, Vol. 1, p. 114.
[82] J.D. Scantlebury and G.A.M. Sussex, in H. Leidheiser (ed.), *Corrosion Control by Coatings*, National Association of Corrosion Engineers, Houston, TX, USA, 1981, p. 51.

[83] J.C. Rowlands and D.J. Chuter, *Proc. 8th Int. Congr. Metallic Corrosion, Mainz, 1981*, p. 1068.
[84] F.M. Geenen, *Ph.D. Thesis*, Delft University of Technology, Netherlands, 1991, p. 77.
[85] B.N. Popov, M.A. Alwahaibi and R.E. White, *J. Electrochem. Soc., 140* (1993) 947.
[86] J.C. Padget and P.J. Moreland, *J. Coat. Technol., 55* (698) (1983) 39.
[87] S. Feliu, J.C. Galvan and M. Morcillo, *Proc. 10th Int. Congr. Metallic Corrosion, Madras, 1987*, p. 1235.
[88] J.C. Galvan, S. Feliu and M. Morcillo, *Prog. Org. Coat., 17* (1989) 135.
[89] G.W. Walter, *Corros. Sci., 32* (1991) 1059.
[90] J.R. Scully, *J. Electrochem. Soc., 136* (1989) 979.
[91] W.S. Tait, *J. Coat. Technol., 61* (768) (1989) 57.
[92] J.H.W. de Wit, *Proc. 12th Int. Corrosion Congr., Houston, TX, 1993*, p. 420.
[93] A. Miszczyk, in J.M. Costa and A.D. Mercer (eds.), *Progress in the Understanding and Prevention of Corrosion*, The Institute of Materials, London, UK, 1993, p. 273.
[94] J. Bordzilowski, in J.M. Costa and A.D. Mercer (eds.), *Progress in the Understanding and Prevention of Corrosion*, The Institute of Materials, London, UK, 1993, p. 279.
[95] G.W. Walter, *Corros. Sci., 32* (1991) 1041.
[96] C.T. Chen and B.S. Skerry, *Corrosion, 47* (1991) 598.
[97] A. Amirudin and D. Thierry, *Br. Corros. J., 26* (1991) 195.
[98] P. Gimenez, D. Petit and M. Badia, *Mater. Sci. Forum, 8* (1986) 315.
[99] N. Kouloumbi, G.M. Tsangaris and S.T. Kyvelidis, *J. Coat. Technol., 66* (839) (1994) 83.
[100] B. Fastrup and A. Saarnak, *Prog. Org. Coat., 16* (1988) 277.
[101] F. Mansfeld, M.W. Kendig and S. Tsai, *Corrosion, 38* (1982) 478.
[102] M.W. Kendig, F. Mansfeld and S. Tsai, *Corros. Sci., 23* (1983) 317.
[103] F. Mansfeld and M. Kendig, in C. Haynes and R. Baboian (eds.), *Electrochemical Impedance Tests for Protective Coatings, ASTM STP 866*, American Society for Testing and Materials, Philadelphia, PA, 1985, p. 122.
[104] M. Kendig and H. Leidheiser, *J. Electrochem. Soc., 123* (1976) 982.
[105] R.D. Armstrong and J.D. Wright, *Corros. Sci., 33* (1992) 1529.
[106] R.D. Armstrong, J.D. Wright and T.M. Handyside, *J. Appl. Electrochem., 22* (1992) 795.
[107] V.K. Miskovic-Stankovic, D.M. Drazic and M.J. Teodorovic, *Corros. Sci., 37* (1995) 241.
[108] J.R. Scully and S.T. Hensley, *CORROSION/93*, National Association of Corrosion Engineers, New Orleans, LA, USA, Paper No. 359.
[109] F. Bellucci, L. Nicodemo, T. Monetta, M.J. Kloppers and R.M. Latanison, *Corros. Sci., 33* (1992) 1203.
[110] J.F. McIntyre and H. Leidheiser, *J. Electrochem. Soc., 133* (1986) 43.
[111] M.D. Maksimovic and V.B. Miskovic-Stankovic, *Corros. Sci., 33* (1992) 271.
[112] R. Touhasent and H. Leidheiser, *Corrosion, 28* (1972) 435.
[113] S. Haruyama, M. Asari and T. Tsuru, in M.W.Kendig and H.Leidheiser (eds.), *Proc. Symp. Corrosion Protection by Organic Coatings*, The Electrochemical Society, USA, 1987, p. 197.
[114] F. Mansfeld and C.H. Tsai, *Corrosion, 47* (1991) 958.
[115] M.W. Kendig, S. Jeanjaquet and J. Lumsden, in J.R. Scully, D.C. Silverman and M.W. Kendig (eds.), *Electrochemical Impedance: Analysis and Interpretation, ASTM STP 1188*, American Society for Testing and Materials, Philadelphia, PA, 1993, p. 407.
[116] L.M. Callow and J.D. Scantlebury, *J. Oil Colour Chem. Assoc., 64* (1981) 119.
[117] L.M. Callow and J.D. Scantlebury, *J. Oil Colour Chem. Assoc., 66* (1983) 93.
[118] F. Deflorian, L. Fedrizzi and P.L. Bonora, in J.M. Costa and A.D. Mercer (eds.), *Progress in the Understanding and Prevention of Corrosion*, Vol. I, The Institute of Materials, London, UK, 1993, p. 215.
[119] J.L. Dawson and D.G. John, *J. Electroanal. Chem., 10* (1980) 37.
[120] I. Sekine, K. Sakaguchi and M. Yuasa, *J. Coat. Technol., 64* (810) (1992) 45.
[121] D.H. van der Weijde, E.P.M. van Westing and J.H.W. de Wit, *Corros. Sci., 36* (1994) 643.
[122] F. Deflorian, L. Fedrizzi and P.L. Bonora, *Corrosion, 50* (1994) 113.
[123] J.N. Murray and H.P. Hack, *CORROSION/92*, National Association of Corrosion Engineers, Nashville, TX, USA, Paper No. 230.
[124] S.A. McLuney, S.N. Popova, B.N. Popov, R.E. White and R.B. Griffin, *J. Electrochem. Soc., 139* (1992) 1556.

[125] A. Amirudin, P. Jernberg and D. Thierry, *Proc. 12th Int. Corrosion Congr., Houston, TX, 1993,* Vol. 1, p. 171.
[126] J.N. Murray and H.P. Hack, *Corrosion, 47* (1991) 480.
[127] H.P. Hack and J.R. Scully, *J. Electrochem. Soc., 138* (1991) 33.
[128] J.N. Murray and H.P. Hack, *Proc. 12th Int. Corrosion Congr., Houston, TX, 1993,* Vol. 1, p. 151.
[129] J.A. Grandle and S.R. Taylor, *Corrosion, 50* (1994) 792.
[130] A. Amirudin, C. Barreau, R. Hellouin and D. Thierry, Evaluation of anti-corrosive pigments by pigment extract-studies, atmospheric exposure and electrochemical impedance spectroscopy, *Prog. Org. Coat., 25* (1995) 339.
[131] T.C. Simpson, H. Hampel, G.D. Davis, C.D. Arah, T.L. Fritz, P.J. Moran, B.A. Shaw and K.I. Zankel, *J. Electrochem. Soc., 136* (1989) 2761.
[132] T.C. Simpson, H. Hampel, G.D. Davis, C.D. Arah, T.L. Fritz, P.J. Moran, B.A. Shaw and K.I. Zankel, *Corrosion, 46* (1990) 331.
[133] T.C. Simpson, H. Hampel, G.D. Davis, C.D. Arah, T.L. Fritz, P.J. Moran, B.A. Shaw and K.I. Zankel, in R. Baboian and S.W. Dean (eds.), *Corrosion Testing and Evaluation, ASTM STP 1000,* American Society for Testing and Materials, Philadelphia, PA, 1990, p. 397.
[134] T.C. Simpson, H. Hampel, G.D. Davis, C.D. Arah, T.L. Fritz, P.J. Moran, B.A. Shaw and K.I. Zankel, *Prog. Org. Coat., 20* (1992) 199.
[135] C. Barreau and D. Thierry, *Rev. Metall., 7* (1990) 457.
[136] A. Al-Hashem and D. Thomas, *J. Coat. Technol., 62* (783) (1990) 51.
[137] A. Amirudin, C. Barreau, D. Massinon and D. Thierry, *Mater. Sci. Forum, 111–112* (1992) 291.
[138] A. Amirudin and D. Thierry, Application of electrochemical impedance spectroscopy to study the atmospheric corrosion of painted metals, *Mater. Sci. Forum,* in press.
[139] A. Amirudin, *Ph.D. Thesis,* The Royal Institute of Technology, Stockholm, Sweden, 1994, p. 59.